Transactions of the Materials Research Society of Japan 30[3] 651-654 (2005)

Photo-patternable Catalyst Surface for Electroless Deposition

Jae-Young Lee, Dehui Yin and Shin Horiuchi
Nanotechnology Research Institute, National Institute of Advanced Industrial Science and Technology (AIST),
1-1-1, Higashi, Tsukuba, Ibaraki 305-8565, Japan
Fax: +81-29-861-4437, e-mail: s.horiuchi@aist.go.jp

Zinc oxide (ZnO) crystal was grown site-selectively on the photo-patternable catalyst surface through electroless deposition process by the reduction of nitrate anion in the aqueous solution of $Zn(NO_3)_2$ with dimethylamine borane. Palladium (Pd) nanoparticles as a photo-patternable catalyst were mainly produced on the UV irradiated poly(methylmethacrylate) (PMMA) region by the reduction of palladium(II) bis(acetylacetonato), so ZnO nanoparticles whose average particle size was 20 times larger than Pd nanoparticles were synthesized on the Pd catalysts site-selectively, which was confirmed by a scanning electron microscopy (SEM) and an energy-filtering transmission electron microscopy (EFTEM) observations. As reaction time increased, the average ZnO particle size increased slightly regardless of UV irradiation, and the surface-covering rate for the UV irradiated regions steeply increased, while that for the UV unirradiated regions slightly increased. The morphology of ZnO crystals was greatly influenced by the reaction temperature: fibrillar (at 30°C and 40°C), sphere-like (at 50°C), and hexagonal shape (at 60°C and 70°C).
Keywords: electroless deposition, zinc oxide, patterning, nanoparticle, palladium catalyst

1. INTRODUCTION

Zinc oxide (ZnO) has been an attractive and promising material in the field of optoelectronics such as transparent conductive devices, solar cell windows, high-resolution field emission display, ultraviolet or blue laser diodes, etc., and new micropatterning techniques for the preparation of ZnO thin film on the various substrates have been investigated [1-4]. There are many well-known methods such as sputtering [5], metal organic chemical vapor deposition (MOCVD) [6], molecular beam epitaxy (MBE) [7] and pulsed laser deposition (PLD) [8], etc. However, these techniques have serious demerits that the deposition condition is too violent to preserve the substrates without damage and it is hard to obtain high-resolution patterning edges in the etching step due to tearing of the ZnO film during the lift-off process [9,10].

To overcome the demerits, electroless deposition technique is concerned, for it is simple, economical and low energy loss process that can be applied at room temperature. To employ this technique, the surface of substrate should be catalyzed to initiate the deposition process. Conventionally, Pd catalyst was produced by dipping a substrate into $SnCl_2$ and $PdCl_2$ aqueous solutions, respectively [11]. Recently, photo-patternable self-assembled monolayers (SAM) have been employed to get patterned Pd catalysts [2,3,12]. UV light passing a photomask changes the UV-sensitive group on the SAM to Pd-attractive group, so Pd catalysts can be selectively attached on the substrate's surface with reproducing the photomask pattern.

We have developed a very simple method to get the patterned Pd catalysts on various polymer thin films by a dry process [13,14]. Palladium(II) bis(acetylacetonato) ($Pd(acac)_2$) complexes penetrate into polymer films in the vapor phase and are reduced to the Pd metals, and then they aggregate in the form of Pd nanoparticles. When a block copolymer was exposed to $Pd(acac)_2$, Pd nanoparticles mainly align on the Pd-attractive microdomains [13]. We found that the reduction rate of PMMA was too low to get sufficient Pd nanoparticles. We also found, however, that the rate was largely increased to form sufficient Pd nanoparticles by the UV irradiation on the PMMA film before incorporation of $Pd(acac)_2$ [14]. In this paper, we report micropatterning of ZnO by combining the UV-assisted Pd patterning on PMMA thin film and the electroless deposition of ZnO on the Pd catalyst.

2. EXPERIMENTAL

2.1 Materials

Palladium(II) bis(acetylacetonato) ($Pd(acac)_2$) complex was purchased from Johnson Matthey Materials Technology. It was purified by the recrystallization in acetone. PMMA was obtained from Aldrich Chemical Company, Inc. whose number-average molecular weight, Mn was 350,000. It was precipitated twice from methylene chloride into methyl alcohol for the purification. Zinc nitrate ($Zn(NO_3)_2$) and dimethylamine borane (DMAB) were purchased from Wako Pure Chemical Industries, Ltd, and silicon wafer was the product of Shin-Etsu Chemical Co., Ltd. in the type of CZ-P.

2.2 Pd Patterning on PMMA thin film

First, PMMA thin film with 20 nm thickness was prepared on the O_2 plasma-cleaned Si wafer (1.5 _ 1.5 _ 0.7 mm^3) by spin coating from 0.75 wt% PMMA/ toluene solution and drying at 60°C for 2hr in vacuum oven. And then, it was treated by UV light at the dose of 10 J/cm^2 through a photomask. The UV irradiation was employed using a spot light source in which a mercury-xenon lamp generated line spectra ranging from 240 to 400 nm with the intensity of 100 mW/cm^2 at 250 nm.

In order to pattern Pd element on UV irradiated region site-selectively by the reduction of $Pd(acac)_2$, the

following procedure was used, as described in our previous paper [13,14]: 5 mg of $Pd(acac)_2$ in the glass reactor was sublimed at 180°C in vacuo and condensed to the upper side of glass wall. Then the PMMA thin film coated on the Si wafer was placed into the glass reactor and maintained at 180°C for 5 min in N_2 atmosphere. In this stage, most of Pd clusters were positioned within the UV patterned area.

2.3 ZnO deposition

To make the ZnO crystals grow on the Pd pattern, 0.05M $Zn(NO_3)_2$ and 0.05M DMAB aqueous solutions were separately heated to the reaction temperature in order to avoid the pre-reaction during the heating to the reaction temperature. Two aqueous solutions were mixed instantly and Pd patterned substrate was soaked into the aqueous solution at 30~70°C for various times.

2.4 Instrumental analyses

Chemical composition of the ZnO was analyzed by X-ray photoelectron spectroscopy (XPS, PHI's Quantum 2000 Scanning ESCA Microprobe). The distribution of Pd nanoparticles was observed by energy-filtering transmission electron microscopy (EFTEM, LEO922) and ZnO morphology was done by scanning electron microscopy (SEM, Philips XL30 FE-SEM). The number of Pd and ZnO nanoparticles, and surface-covering rate by ZnO were estimated by an image processing software (analySIS, Soft Imaging System Co. Ltd.).

3. RESULTS AND DISCUSSION

To observe the patterning of Pd nanoparticles, PMMA film was spin-coated on a cleaved NaCl crystal and it was UV irradiated through photomask. And then it was exposed to the $Pd(acac)_2$ vapor, as following the similar procedure of the experimental section. After the exposure, the Pd patterned PMMA film was lifted-off from the substrate by dipping it into water and was mounted on a 600 mesh TEM copper grid, which was preliminary coated with carbon film by dipping the carbon coated NaCl into water.

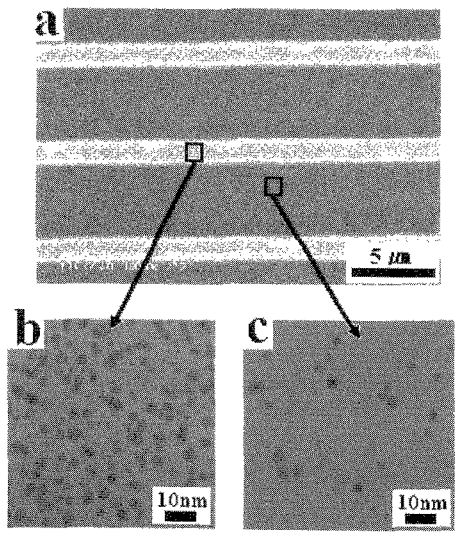

Fig.1 (a) SEM image showing Pd patterning on UV patterned PMMA thin film, and magnified TEM images from (b) UV irradiated and (c) UV unirradiated regions.

A low magnification view by SEM image in Fig.1a reproduced the photomask pattern, and the magnified TEM images from the irradiated and the unirradiated regions (Fig.1b and 1c, respectively) showed the significant difference in the number of the Pd nanoparticles, where black dot was the Pd catalysts in the nanocluster form. The distribution density of Pd nanoparticles in the UV irradiated region was far higher than that of unirradiated region. It was due that the C=C double bond coming from the breakage of PMMA main chain by UV stimulation maybe enhanced the reduction rate of $Pd(acac)_2$ to metallic Pd catalyst [13]. The number of Pd nanoparticles and its number-average diameter in the UV irradiated regions were 52 particles/1,000 nm^2 and 2.4 nm, respectively, and those in the UV unirradiated regions were 8 particles/1,000 nm^2 and 2.2 nm, respectively. The nanoparticle size was almost same, but the number was very different.

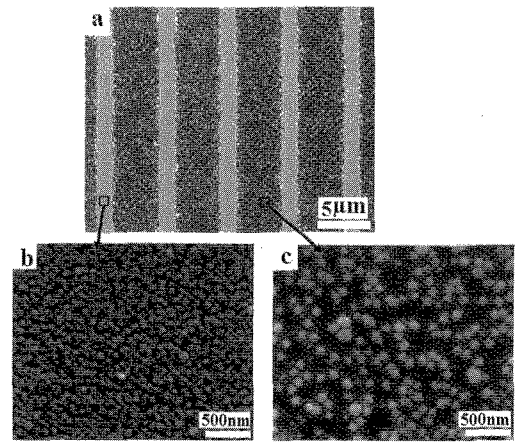

Fig.2 SEM images for ZnO micropatterning fabricated on the Pd patterned PMMA thin film at 50°C for 10 min. (a) ZnO patterning, (b) ZnO nanoparticles generated in the UV irradiated region and (c) those generated in the UV unirradiated region.

SEM image in Fig.2a showed the well-arranged micropatterning on the PMMA thin film synthesized at 50°C for 10 min in an aqueous solution of 0.05M $Zn(NO_3)_2$ and 0.05M DMAB. The contrast between the irradiated and the unirradiated regions was significantly enhanced through the deposition process, suggesting that most ZnO was deposited with an excellent site-selectivity on the white regions, which were precisely fitted with the UV patterned regions.

Fig.2b and 2c showed the SEM images of ZnO nanoparticles generated in the UV irradiated and unirradiated regions, respectively. Obviously, ZnO nanoparticles covered almost all the surface of the UV irradiated region forming a dense continuous film, while very few nanoparticles grew on the UV unirradiated region. However, the shape of the nanoparticles in the two regions was sphere-like without regard to UV treatment. In order to estimate the average particle size and the surface-covering rate by ZnO, these SEM images were introduced to the image processing software. The average particle size was measured in very similar size regardless of UV irradiation, which were 52.9 nm and 54.2 nm for UV irradiated and unirradiated region, respectively. However, surface-

covering rate, 81.9 % for UV irradiated region was remarkably different from 26.5 % for UV unirradiated region. The smaller ZnO particles and the more dense deposition were obtained in our process with the remarkably shorter deposition times in comparison with the other previous works with the conventional catalyst based on $PdCl_2$ and $SnCl_2$ [2,15].

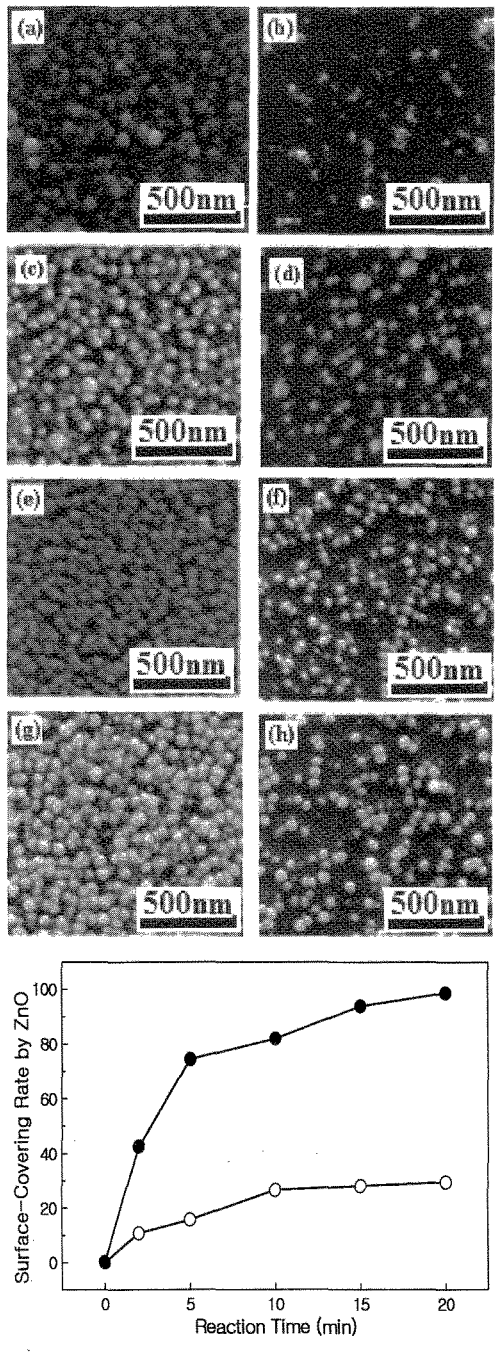

Fig.3 SEM images of ZnO particles prepared at 50°C for (a,b) 2 min, (c,d) 5 min, (e,f) 10 min, and (g,h)20 min, respectively, where left sides were for the UV irradiated regions and right ones were for the UV unirradiated regions; Graph shows surface-covering rate according to reaction time, where(●)UV irradiated region and (○)UV unirradiated region.

With the help of XPS analysis, we confirmed that the deposited particles were ZnO, for the XPS characteristic peaks of Zn2*p* were found at 1045.5 eV for $Zn2p_{1/2}$ and 1022.3 eV for $Zn2p_{3/2}$, which was in good agreement with the typical ZnO film [16]. The elemental maps of zinc and oxygen by EFTEM [17] precisely overlapped on the deposited ZnO particles, which also verified that the deposited particles were ZnO.

Fig.3a-3h show SEM images for ZnO nanoparticles generated at the UV irradiated and unirradiated regions in the line micropatterning, respectively, which were produced at 50°C for various times in the aqueous solution of 0.05M $Zn(NO_3)_2$ and 0.05M DMAB. ZnO nanoparticles successfully covered almost all the surface of the UV irradiated region, while very few ones distributed on the UV unirradiated region, since the dense of Pd catalyst inclined to the UV irradiated region. The shape of the nanoparticles in the two regions was sphere-like without regard to UV treatment and reaction time. In order to measure the average particle size and the surface-covering rate, the SEM images were introduced to image processing software. As reaction time increased from 2 min to 20 min, the average particle size for UV irradiated and unirradiated regions increased slightly from 47.0 nm to 54.4 nm and from 47.6 nm to 58.1 nm, respectively, which were about 20 times higher than that of Pd nanoparticle. The surface-covering rate for the UV irradiated regions steeply increased from 42.5% to 98.6% with increasing reaction time, while that for the UV unirradiated regions gently increased from 10.7% to 29.4%, as shown in Fig.3.

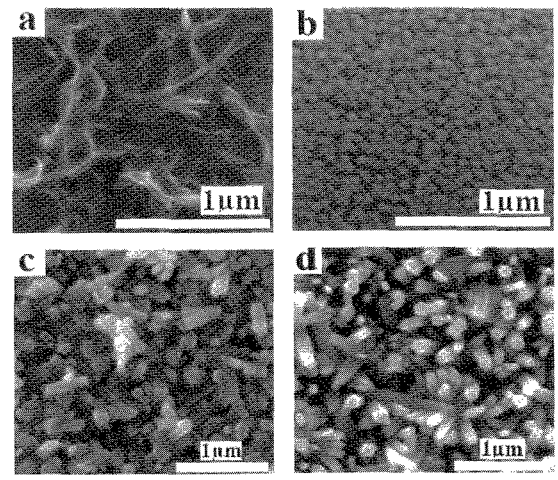

Fig.4 SEM images for ZnO deposited on the Pd patterned PMMA thin film at various temperatures for 20 min: (a) 40°C, (b) 50°C, (c) 60°C and (d) 70°C

Fig.4 shows the SEM images of the surface of the ZnO film deposited on the UV irradiated region, which was synthesized at various temperatures for 20 min in the aqueous solution of 0.05M $Zn(NO_3)_2$ and 0.05M DMAB. The morphology of ZnO synthesized at 40°C was fibrillar shape (Fig.4a) and the ZnO film of 30°C was also of similar fibrillar shape, which was not shown. The morphology of ZnO synthesized at 50°C was of sphere-like (Fig.4b) nanoparticles as was shown in Fig.3, while those grown at 60°C and 70°C were of relatively uniform hexagonal shape (Fig.4c and 4d, respectively). The comparison of the SEM images revealed that the

morphology of the ZnO thin films changed greatly with the increasing reaction temperature.

4. CONCLUSIONS

A simple site-selective deposition method for the Zinc oxide (ZnO) on Pd patterned PMMA thin film through an electroless process was developed by the reduction of nitrate anion in the aqueous solution of $Zn(NO_3)_2$ with dimethylamine borane. EFTEM analysis showed that most Pd nanoparticles were generated in the UV irradiated region and ZnO nanoparticles were synthesized on the Pd catalysts site-selectively, which was confirmed by XPS and SEM techniques. On a XPS spectrum, the characteristic peaks of Zn 2*p* were found at 1045.5 eV and 1022.3 eV for Zn $2p_{1/2}$ and Zn $2p_{3/2}$, respectively, which was in good agreement with the typical ZnO films. The elemental maps of zinc and oxygen by EFTEM confirmed that the deposited particles were ZnO. ZnO nanoparticles covered almost all the surface of the UV irradiated region forming a dense continuous film, while very few nanoparticles grew on the UV unirradiated region, which made it possible to get excellent micropatterning of ZnO. The surface-covering rate by ZnO for the UV irradiated regions steeply increased from 42.5% to 98.6% with increasing reaction time, while that for the UV unirradiated regions gently increased from 10.7% to 29.4%. The more dense deposition were obtained in this process with the remarkably shorter deposition times in comparison with the other previous works with the conventional catalyst based on $PdCl_2$ and $SnCl_2$. The morphology of ZnO structures was greatly influenced by the reaction temperature: fibrillar (at 30°C and 40°C), sphere-like (at 50°C), and hexagonal shape (at 60°C and 70°C).

ACKNOWLEDGEMENT

The financial support by New Energy and Industrial Technology Development (NEDO) for the Nanostructured Polymer Project is greatly acknowledged. J. Y. Lee thanks Japan Society for the Promotion of Science (JSPS) for the post doctoral fellowship.

REFERENCES

[1] M. H. Huang, S. Mao, H. Feick, H. Yan, Y. Wu, H. Kind, E. Weber, R. Russo and P. Yang, *Science*, 292, 1897-1899 (2001).
[2] N. Saito, H. Haneda, T. Sekiguchi, N. Ohashi, I. Sakaguchi and K. Koumoto, Adv. Mater., **14**, 418-421 (2002).
[3] M. S. Chen, S. L. Brandow and W. J. Dressick, Thin Solid Films, **379**, 203-212 (2000).
[4] G. H. Lee, Y. Yamamoto, M. Kourogi and M. Ohtsu, Thin Solid Films, **386**, 117-120 (2001).
[5] D. H. Zhang, T. L. Yang, Q. P. Wang and D. J. Zhang, Mater. Chem. Phys., **68**, 233-238 (2001).
[6] S. Muthukumar, H. Sheng, J. Zhong, Z. Zhang, N. W. Emanetoglu and Y. Lu, IEEE Trans. Nanotech., **2**, 50-54 (2003).
[7] C. R. Gorla, N. W. Emanetoglu, S. Liang, W. E. Mayo, Y. Lu, M. Wraback and H. Shen, J. Appl. Phys., **85**, 2595-2602 (1999).
[8] R. D. Vispute, V. Talyansky, S. Choopun, R. P. Sharma, T. Venkatesan, M. He, X. Tang, J. B. Halpern, M. G. Spencer, Y. X. Li, L. G. Salamanca-Riba, A. A. Iliadis and K. A. Jones, J. Appl. Phys., **73**, 348-350 (1998).
[9] Y. G. Wang, S. P. Lau, H. W. Lee, S. F. Yu, B. K. Tay, X. H. Zhang and H. H. Hng, J. Appl. Phys., **94**, 354-358 (2003).
[10] S. O. Kucheyev, P. N. K. Deenapanray, C. Jagadish, J. S. Williams, M. Yano, K. Koike, S. Sasa, M. Inoue and K. I. Ogata, J. Appl. Phys., **81**, 3350-3352 (2002).
[11] I. Lee, P. T. Hammond and M. F. Rubner, Chem. Mater., **15**, 4583-4589 (2003).
[12] T. N. Khoperia, T. J. Tabatadze, T. I. Zedgenize, Electrochim. Acta., **42**, 3049-3055 (1997).
[13] S. Horiuchi, T. Fujita, T. Hayakawa and Y. Nakao, Langmuir, 7, 2963-2973 (2003).
[14] S. Horiuchi, M. I. Sarwar and Y. Nakao, Adv. Mater., **15**, 1449-1452 (2003).
[15] M. Izaki and J. Katayama, J. Electrochem. Soc., **147**, 210-213 (2000).
[16] N. Islam, T. B. Ghosh, K. L. Chopra and H. N. Acharya, Thin Solid Films, 280, 20-25 (1996).
[17] L. Reimer, "Energy-Filtering Transmission Electron Microscopy", Ed. by L. Reimer, Springer Münster (1995) pp. 347-400.

(Received December 23, 2004; Accepted April 14, 2005)